Progress In Electromagnetics Research C, Vol. 7, 65–78, 2009

TUNABLE LOWPASS FILTERS USING FOLDED SLOTS ETCHED IN THE GROUND PLANE

G. Ramzi, Z. Hassen, H. Trabelsi, and H. Baudrand †

Department of Physics, Faculté des Sciences de Tunis
Electronics Laboratory
2092 El Manar, Tunisia

Abstract—This paper presents a new concept to implement tunable lowpass filters by employing slot resonators etched in the ground plane. The tenability is achieved with the use of switches with varactor diodes attached across the slots on the ground.

The concept is demonstrated by considering 10-slots lowpass and 4-slots low pass filters.

The Microstrip lines with a folded slot etched in the ground plane structure are modelled in multilayered media. To analyze this type of structure an iterative method based on the concept of waves is developed and adapted to determine features of very high frequency's electronic circuits in a planar wave guide.

The analysis takes into account eventual coupling parasites. Experimental measurements are performed to validate the computation. The approach involves the mixed magnetic and electric filed equation technique and the wave concept iterative process which involves S-parameters extraction technique. In this sense, a program in FORTRAN has been elaborated to determine different parameters S_{ij} characterizing the studied structure.

1. INTRODUCTION

Electromagnetic Band Gap (EBG) structures have become very popular as well as an active area of research in the microwave and antenna communities. The EBGs are a new type of engineered materials that exhibit well defined stop and pass bands in the transmission characteristics and as such they find many applications

Corresponding author: G. Ramzi (Gharbi.ramzi@gmail.com).
† G. Ramzi, Z. Hassen, and H. Trabelsi are also with Recherche et concept en Electromagnetism, RCEM, 17 rue Denis Papin, Toulouse 31217, France.

in microwave printed circuit filters, and antennas. A good fraction of these developments involves the ground planes printed with various patterns, slots and cuts.

In this paper, we propose a simple design of a microstrip filter employing EBG structures in the form of folded slot etched on the ground plane, and a new design of the tunable lowpass filters by inserting a lamped element in the ground. The proposed configuration is modelled in multilayered media, and analyzed by a new method based on the Multilayer Contribution of Wave Concept Iterative Process (MLC-WCIP). The MLC-WCIP method are developed and adapted in but to resolve this type of structure. This approach involves the mixed magnetic and electric field equations technique and the wave concept iterative process which involves S_{ij} parameters extraction technique. Theoretical approach is compared with experimental measurements to validate the calculations.

Theoretical approach is compared with experimental measurements to validate the calculations.

2. FORMULATION OF THE MULTILAYER CONTRIBUTION OF THE WCIP METHOD

The wave concept is introduced to express the boundary conditions on the interface air/dielectric in terms of waves [5, 6]. An electric field source E_0 is defined to initialize the iterative process. This source is defined on the discontinuity plane Ω in each port. So, two spatial waves with two components A_1 and A_2 are generated by the upper and lower cover of a metallic box giving two spectral waves B_1 and B_2, which come back to the dielectric interface producing the waves for the next iteration. The incident and reflected waves can be expressed as a function of the electric field E_p and current density J_p at the plane Ω. It leads to the following set of equations:
Z_0 is the equivalent impedance between the two regions given as:

$$Z_0 = \frac{Z_{01} Z_{02}}{Z_{01} + Z_{02}} \tag{1}$$

Z_{0i} is the characteristic impedance of region 1 given by $Z_{0i} = \sqrt{\frac{\mu_0}{\varepsilon_0 \varepsilon_r}}$ where ε_i, μ_i are the permittivity and permeability of region I respectively.

The boundary condition on the sources can be written as:

$$E_1 = E_2 = E_0 - Z_0(J_1 + J_2) \tag{2}$$

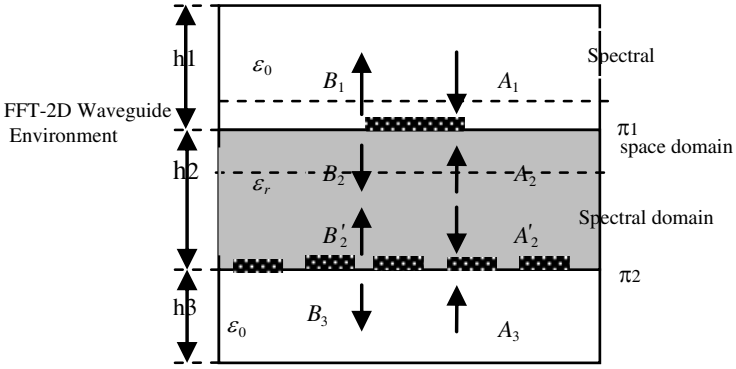

Figure 1. EGB structure modelled in MLC-WCIP.

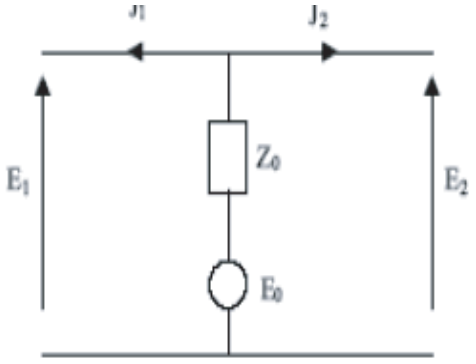

Figure 2. Equivalent circuit of the interface air-dielectric.

The wave's concept is introduced by writing the electric field E_i and the current J_i in terms of waves. It leads to the following set of equation:

$$\vec{E_i} = \sqrt{Z_{0i}}\left(\vec{A_i} + \vec{B_i}\right) \tag{3a}$$

$$\vec{J_i} = \frac{1}{\sqrt{Z_{0i}}}\left(\vec{A_i} - \vec{B_i}\right) \tag{3b}$$

where $Z_{0i} = \sqrt{\frac{\mu_0}{\varepsilon_0 \varepsilon_r}}$.

Using Equations (2), (3), (4) and referring to [7] it is possible to determine the diffraction operator [1] (in space domain) characterizing

the behaviour of waves at interface

$$S_{12}=\begin{bmatrix} H_m+\dfrac{-1+n_1-n_2}{1+n_1+n_2}+\dfrac{1-n^2}{1+n^2}Hs & \dfrac{2n}{1+n^2}H_d+\dfrac{2m}{1+n_1+n_2}Hs \\ \dfrac{Z_n}{1+n^2}H_d+\dfrac{2m}{1+n_1+n_2}Hs & H_m+\dfrac{1-n^2}{1+n^2}H_d+\dfrac{-1-n_1+n_2}{1+n_1+n_2}Hs \end{bmatrix} \tag{4}$$

where:

$H_m = 1$ on the metal and 0 elsewhere.

$H_d = 1$ on the dielectic and 0 elsewhere.

$H_s = 1$ on the source and 0 elsewhere.

$$n=\sqrt{\frac{Z_0}{Z_{02}}},\quad m=\frac{Z_0}{\sqrt{Z_{01}Z_{02}}},\quad n_1=\frac{Z_0}{Z_{01}},\quad n_2=\frac{Z_0}{Z_{02}}$$

The region on both sides of π is designed by region 1 and region 2, where higher-order modes are shunted by their reactive admittance Y.

Thus, it is possible to define a reflection operator in modes. The reflected wave A_i can be obtained:

$$B^\alpha = \sigma_i^\alpha A_i^\alpha \tag{5}$$

with $i = 1$ or 2, $\alpha =$ Is the TE or TM mode.

$$\begin{aligned} \sigma_i^\alpha &= \frac{1-Z_{0i}Y_{im,n}^\alpha \mathrm{Coth}(Y_{im,n}h_i)}{1+Z_{0i}Y_{im,n}^\alpha \mathrm{Coth}(Y_{im,n}h_i)} \\ Y_{im,n}^{TE} &= \frac{\gamma_{im,n}}{j\omega\mu} \qquad Y_{im,n}^{TM}=\frac{j\omega\varepsilon}{\gamma_{im,n}} \\ \gamma_{im,n}^2 &= \left(\frac{m\pi}{a}\right)^2+\left(\frac{n\pi}{b}\right)^2-k_0^2\varepsilon_{ri} \end{aligned} \tag{6}$$

K_0 is the space number.

We note that to calculate the reflected waves in A_i^α, B_i^α spectral domain, it is well known that a 2d FFT in waveguide environment is done [1, 2].

This transformation is expressed as:

$$\begin{bmatrix} A_1^{TE} \\ A_2^{TE} \\ A_1^{TM} \\ A_2^{TM} \end{bmatrix} = K_m \begin{bmatrix} -\dfrac{m}{a} & 0 & \dfrac{n}{b} & 0 \\ 0 & -\dfrac{m}{a} & 0 & \dfrac{n}{b} \\ \dfrac{n}{b} & 0 & -\dfrac{m}{a} & 0 \\ 0 & \dfrac{n}{b} & 0 & -\dfrac{m}{a} \end{bmatrix} \begin{Bmatrix} FFT\cos\sin\left(A_z^1\right) \\ FFT\cos\sin\left(A_z^2\right) \\ FFT\cos\sin\left(A_z^3\right) \\ FFT\cos\sin\left(A_z^4\right) \end{Bmatrix} \tag{7}$$

with

$$K_{mn} = \sqrt{\frac{ab}{2\sigma_{mn}}} \frac{1}{\sqrt{\left(\frac{m}{a}\right)^2 + \left(\frac{n}{b}\right)^2}}$$

$$\sigma_{mn} = \begin{cases} 2 & \text{if } m, n \neq 0 \\ 1 & \text{if } m, n = 0 \end{cases}$$

Moreover to return into the spatial domain an inverse Fast Fourier Transformation (FFT-2D) must be done [7].

Analysis of tow region

The multilayered structure can be modulated by an equivalent circuit illustrated in Figure 3.

The two network port represents the dielectric between the conductors in the planes $\pi 1$ and $\pi 2$.

Y_1 is the admittance of the upper metal box in the plan $\pi 1$. Y_3 is the admittance of the low metal box in the plane $\pi 2$.

According to Figure 3, it is possible to establish the following equations:

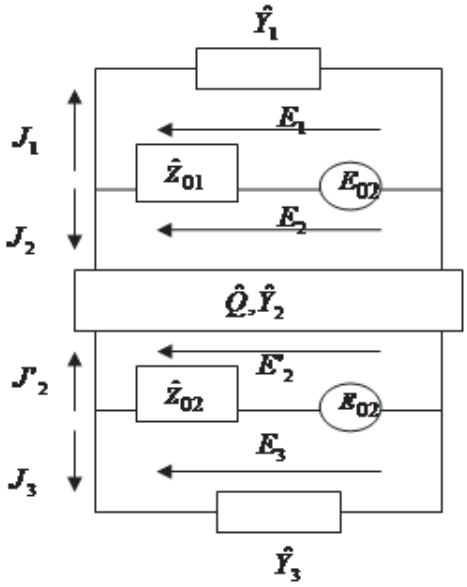

Figure 3. Equivalent circuit.

Space domain

$$\begin{bmatrix} B_{1x,y} \\ B_{2x,y} \end{bmatrix}^{(n)} = [S_{d12}] \begin{bmatrix} A_{1x,y} \\ A_{2x,y} \end{bmatrix}^{(n)} + \begin{bmatrix} B_{01} \\ B_{02} \end{bmatrix} \tag{8}$$

$$\begin{bmatrix} B'_{2x,y} \\ B_{3x,y} \end{bmatrix}^{(n)} = [S_{d23}] \begin{bmatrix} A'_{2x,y} \\ A_{3x,y} \end{bmatrix}^{(n)} + \begin{bmatrix} B'_{02} \\ B_{03} \end{bmatrix} \tag{9}$$

S_{d23} has the same experience as S_{d23}
Spectral domain

$$\begin{bmatrix} A_{1m,n} \\ A_{3m,n} \end{bmatrix}^{(n)} = \begin{bmatrix} \sigma_1^{\alpha} & 0 \\ 0 & \sigma_3^{\alpha} \end{bmatrix} \begin{bmatrix} B_{1m,n} \\ B_{3m,n} \end{bmatrix}^{(n-1)} \tag{10}$$

$$\begin{bmatrix} A_{2m,n} \\ A'_{2m,n} \end{bmatrix}^{(n)} = [\sigma_Q] \begin{bmatrix} B_{2m,n} \\ B'_{2m,n} \end{bmatrix}^{(n-1)} \tag{11}$$

σ_1, σ_3: reflected operator in the spectral domain.

σ_Q: is the admittance operator of the network port.

The Q two ports network can be characterized by referring to the theory of the transmission lines. So the electric model can be represented in Figure 4.

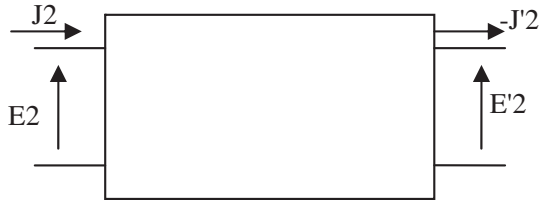

Figure 4. Electric model.

In this way, after some mathematically manipulation, it possible to determine the transmission matrix:

$$\begin{bmatrix} E_2 \\ J_2 \end{bmatrix} = [M] = \begin{bmatrix} \cosh(\gamma h_2) & Z_2 \sin(\gamma h_2) \\ \dfrac{\sin(\gamma h_2)}{Z_{02}} & \cosh(\gamma h_2) \end{bmatrix} \begin{bmatrix} E'_2 \\ -J'_2 \end{bmatrix} \tag{12}$$

M_0: is the transmission matrix. Then using Equations (11), (12) the reflection operator σ_Q can defined as:

$$[\sigma_Q] = \sum_{m,n} \begin{bmatrix} \left|f^{\alpha}_{m,n}\right\rangle \dfrac{A \sinh(\gamma_{m,n} h_2)}{H} \left\langle f^{\alpha}_{m,n}\right| & \left|f^{\alpha}_{m,n}\right\rangle \dfrac{2 Z_2 \sqrt{Z_{01} Z_{02}}}{H} \left\langle f^{\alpha}_{m,n}\right| \\ \left|f^{\alpha}_{m,n}\right\rangle \dfrac{2 Z_2 \sqrt{Z_{01} Z_{02}}}{H} \left\langle f^{\alpha}_{m,n}\right| & \left|f^{\alpha}_{m,n}\right\rangle \dfrac{A \sinh(\gamma_{m,n} h_2)}{H} \left\langle f^{\alpha}_{m,n}\right| \end{bmatrix}$$

with

$$A = Z_2^2 - Z_{01}Z_{02}$$
$$H = 2Z_2\sqrt{Z_{01}Z_{02}}\cosh(\gamma_{m,n}h_2) + \left(Z_2^2 + Z_{01}Z_{02}\right)\sinh(\gamma_{m,n}h_2)$$

$\left|f_{m,n}^{\alpha}\right\rangle$ are the bases function of box modes.

3. CONCEPT OF TUNABLE SLOT RESONATORS

Microstrip lines with a folded slot etched in the ground plane have exhibited a stopband-passband and lowpass filter characteristic and a slow wave effect. These features can be used in lowpass filter application to eliminate unwanted frequencies and to reduce the physical size of microstrip circuits. The design of the proposed filters is based on a more accurate with choosing the dimension of the Microstrip lines with a folded slot etched in the ground plane.

The resonant frequency of the structure is determined by the two factors reflected gap distance g and area (i.e., $a \times b$) of the T-shaped metal-loading.

Therefore, by choosing suitable dimensions of the folded slots, the performance of the microwave circuit, employing this kind of structure, is easily controlled.

The schematic of a 50 Ω microstrip line with a folded slot etched in the ground plane [8] is shows in Figure 5 and the frequency response of this structure in Figure 6. The structure exhibits a passband-stopband property [8].

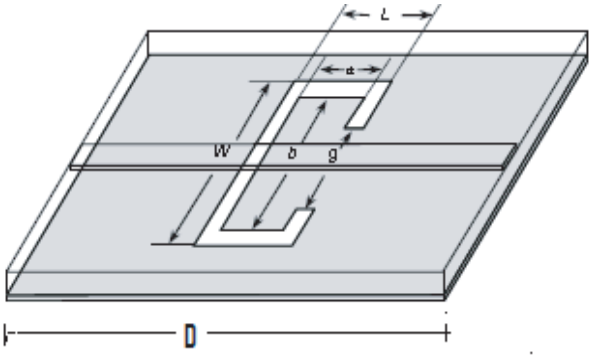

Figure 5. Schematic of a 50 Ω microstrip line with a folded slot etched in the ground plane, $W = 6.096$, $D = 3.9$, $L = 1.524$, $g = 3.048$, $a = 1.016$, $b = 5.6$, $h = 0.635$, $\varepsilon r = 10.6$, F resonate = 6.8 GHz.

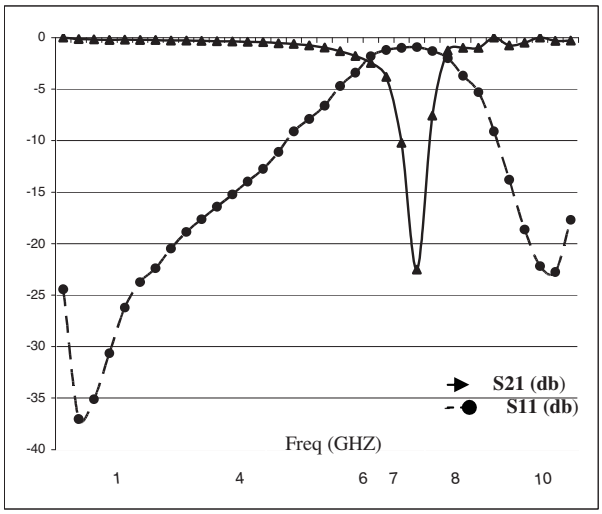

Figure 6. The frequency response of the 50 Ω microstrip line with a folded slot etched in the ground plane represented in Figure 5 using MLC-WCIP method.

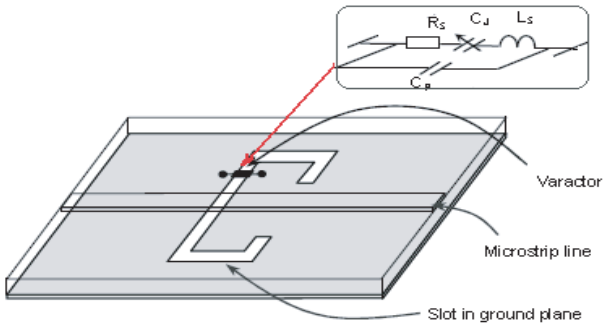

Figure 7. Analogue tunable slot resonator with a varactor diode on the ground plane.

A tunable slot resonator with a varactor diode is presented in Figure 7.

In this section, a tunable slot resonator is presented by employing the varactor diode in the folded slot resonator; then the varactor diode must be modulated by a multilayer concept.

The varactor diodes are MDT with a series resistance of 4 Ω, a series inductance of 1.0 nH, and a package capacitance of $C_p = 0.15$ pF junction capacitance C_j varies from 0.2 pF to 0.7 pF over 25 V bias

range, each varactor is biased with a 100 pF DC bloc capacitor.

The variable capacity used in varactor diode has following expression:

$$C(v) = \frac{C_j}{\left[1 + \dfrac{v}{v_j}\right]^n} \tag{13}$$

C_j is junction capacitance varied from 0.2 pF to 0.7 pF over a 25 V bias range,

v_j is constant when $v_j = 0.7$ volt, $n = 0.5$.

In the lumped element domain, the boundary conditions to be verified are given by:

$$J_s = J_{s1} + J_{s2} \qquad E = E_1 = E_2 = J_s Z_s \tag{14}$$

where Z_s is the surface impedance related to the varactor diode impedance Z_l via.

$$Z_s = \frac{W_s}{L_s} Z_l \tag{15}$$

W_s and L_s are the width and the length of the varactor diode domain respectively.

The relation determined by Equation (14) is traduced in the terms of incident (A) and reflected (B) waves using Equation (3a) and Equation (3b) by the flowing equation:

$$\begin{cases} (A'_2 + B'_2) = \dfrac{\sqrt{Z_{02}}}{\sqrt{Z_{01}}}(A_3 + B_3)_{x,y} \\ (A_3 + B_3)_{x,y} = \dfrac{Z_s}{\sqrt{Z_{02}}} \left\{ \dfrac{1}{\sqrt{Z_{01}}} \left(A'_2 - B'_2\right)_{x,y} + \dfrac{1}{\sqrt{Z_{01}}}(A_3 + B_3)_{x,y} \right\} \end{cases} \tag{16}$$

The used (16) in the (3) results the scattering operator of the lumped element domain:

$$\begin{vmatrix} \vec{B}'_2 \\ \vec{B}_3 \end{vmatrix} = \begin{bmatrix} \dfrac{-Z_{01}Z_{02} - Z_S Z_{01} + Z_S Z_{02}}{Z_{01}Z_{02} + Z_S Z_{01} + Z_S Z_{02}} & \dfrac{2Z_S\sqrt{Z_{01}Z_{02}}}{Z_{01}Z_{02} + Z_S Z_{01} + Z_S Z_{02}} \\ \dfrac{2Z_S\sqrt{Z_{01}Z_{02}}}{Z_{01}Z_{02} + Z_S Z_{01} + Z_S Z_{02}} & \dfrac{-Z_{01}Z_{02} - Z_S Z_{01} + Z_S Z_{02}}{Z_{01}Z_{02} + Z_S Z_{01} + Z_S Z_{02}} \end{bmatrix} \begin{vmatrix} \vec{A}'_2 \\ \vec{A}_3 \end{vmatrix}$$

Now the relation needs to apply in MLC-WCIP algorithm and this structure simulated.

The tunable slot resonator is modulated and analysed by a MLC-WCIP, now we must determinate the sensibility of the frequency response of this structure by varying the junction capacitance C_j of the varactor diode is shown in Figure 8. It can be seen that the resonant frequency is shifted by more than 1.4 GHz by varying the junction capacitance C_j from 0.2 pF to 0.7 pF.

4. APPLICATION TO MICROSTRIP LOWPASS FILTERS

Since single folded slot resonator presents both the cutoff (lowpass) and the resonance (bandstop) characteristic, microstrip lowpass filter can realized by cascading a specified number of such slot resonators. The proposed concept can be used to implement higher order lowpass filters. Figure 8 shows a schematic of a typical microstrip lowpass filter having ten slot resonators etched on the ground plane [9]. The frequency response of this filter is shown in Figure 9.

The simulated of the lowpass filters by iterative method MLC-WCIP exhibit an excellent agreement with a remarkable range performance. Now the lowpass filter can be replaced by the newly developed tunable lowpass filter demonstrated in the next section.

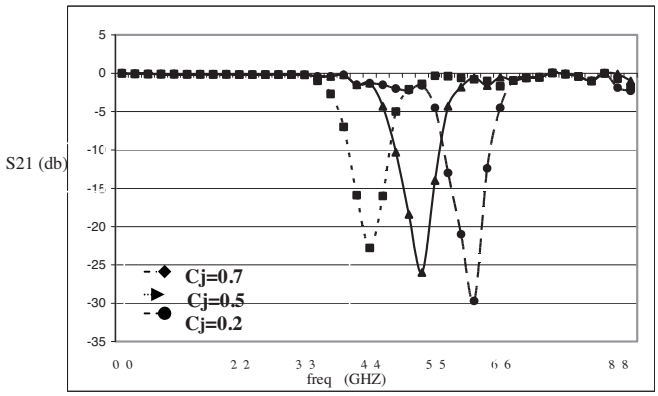

Figure 8. Simulation of the transmission coefficient of a tunable slot resonator shown in Figure 7.

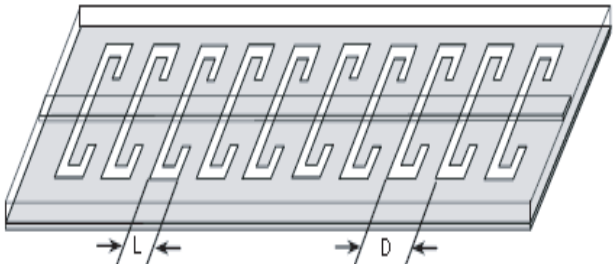

Figure 9. Microstrip low pass filter employing slot on ground plane.

5. TUNABLE LOWPASS FILTERS

This section presents a new concept for implementing tunable lowpass filter by employing proposed tunable folded slot resonators etched on the ground plane. The tuning is achieved by employing MDT varactors diode in slots in the ground plane. The proposed structure are analysed by the MLC-WCIP method.

The analogue tunable filter, as illustrated in Figure 11.

Four varactor diode are mounted on the ground plane in the same manner as RF MEMS switches of digital tunable 4-slot lowpass filter. The varactor diodes are MDT with a series resistance of 4 Ω, a series inductance of 1.0 nH, and a package capacitance of 0.15 pF junction

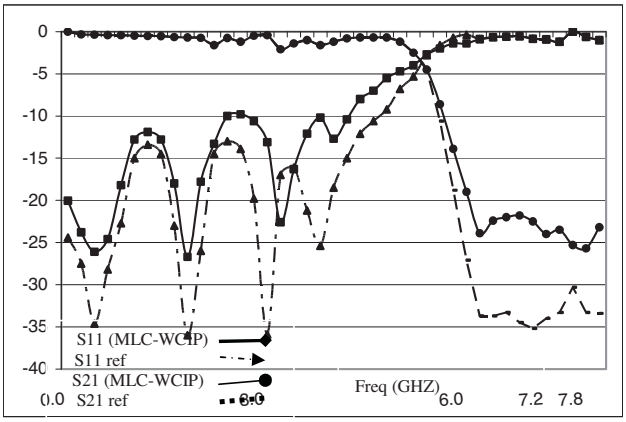

Figure 10. Frequency response of the microstrip low pass filter using MLC-WCIP method.

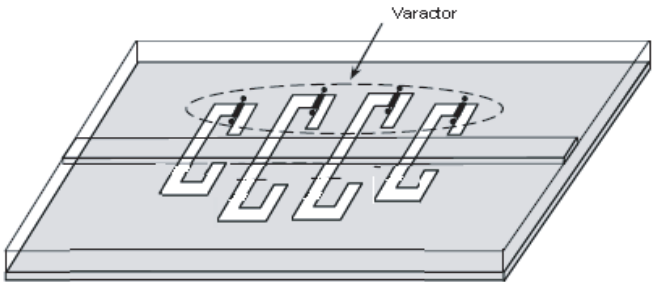

Figure 11. Analogue tunable filter with a 4-varactor diode on the ground plane.

capacitance C_j varies from 0.2 pF to 0.7 pF over 25 V bias range, each varactor is biased with a 100 pF DC bloc capacitor, the four varactors are then connected one to another a wire bond, such that only one DC bias is needed for operating the entire circuit.

The simulation of the S-parametre of the analogue tunable lowpass filter is shown in Figure 12. The previous simulation of using MLC-WCIP method validates the proposed concept of implementing tunable lowpass filter and providing a size reduction and a better RF performance than those traditional EBG structure.

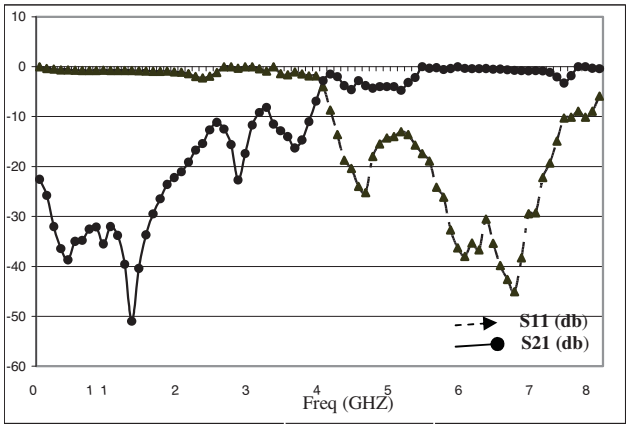

Figure 12. Frequency response of the tunable microstrip low pass filter using MLC-WCIP method.

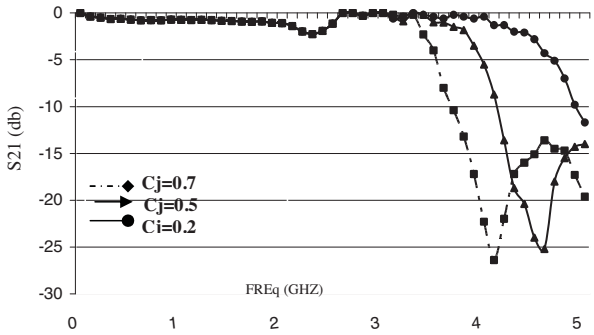

Figure 13. Simulated transmission coefficient of the analogue tunable lowpass filter with the different varactors diode (using MLC-WCIP method).

The simulation results illustrated in Figure 13 depicts the transmission coefficients of the analogue tunable lowpass filter as a function of the applied varactor bias voltage and representing the relation between the variability of the junction capacitance C_j value and a cutoff frequency of the related filter. The theoretical tuning range is from 3.7 GHz ($C_j = 0.5$ pF) to 4.6 GHz ($C_j = 0.2$ pF). The simulation response of the filter presents a tuning range from 3.6 GHz to 4.4 GHz with all varactors biased equally in parallel. The results clearly indicate that the agreement between the simulation results and theoretical prediction. The simulation results prove that by varying the voltage applied to the varactor diodes over a 25 V bias range, a tuning range of 0.8 GHz is achievable without performance degradation in the passband.

6. CONCLUSION

Analogue tunable lowpass a filter has been implemented by cascading several varactor tuned slot resonators is presented in this paper. The tuning range is principally determined by both the value of the variable capacitance of the varactor diode attached in the ground plane. The Analogue tunable lowpass a filter presented good rejection and a large tuning range.

To predict the performance of the tunable lowpass filters, this structure is modelled in multilayered media and analysis by the MLC-WCIP method. The simulation results by the MLC-WCIP method for the tunable lowpass filters confirm a remarkable RF performance with wide tuning range and present a good agreement with experimental measurement.

REFERENCES

1. Gharsallah, A., R. Garcia, A. Gharbi, and H. Baudrand, "Wave concept iterative merges with model fast Fourier transformation to analyze micro-strip filters," *Applied Computed Electromagnetic Society*, Vol. 14, No. 1, 61–67, March 2001.
2. Hong, J. S. and M. J. Lancaster, "Design of highly selective microstrip bandpass filters with a single pair of attenuation poles at finite frequencies," *IEEE Transactions on Microwave Theory and Techniques*, Vol. 48, No. 7, 1098–1107, July 2000.
3. Gharsallah, A., A. Gharbi, L. Desclos, and H. Baudrand, "Analysis of interdigital capacitor and quasi-lumped miniaturized filters using iterative method," *Int. Journal of Numerical*

Modeling: Electronic Networks, Devices and Fields, Vol. 15, 169–179, 2002.

4. Gharsallah, A., A. Gharbi, and H. Baudrand, "Efficient analysis of multiport passive circuitsusing the iterative technique," *Electromagnetics*, Vol. 21, 73–84, 2001.
5. Trabelsi, H., A. Gharsallah, and H. Baudrand, "Analysis of microwave circuits including lumped elements based on iterative method," *International Journal of RF and Microwave Computer-aided Engineering*, Vol. 13, No. 4, 269–275, 2003.
6. Edwin, K., L. Young, J. C. Beal, and Y. M. M. Antar, "Multilayer microstrip structure analysis with matched load simulation," *IEEE Transactions on Microwave Theory and Techniques*, Vol. 43, No. 1, January 1995.
7. Kaddour, M., A. Mami, A. Gharsallah, A. Gharbi, and H. Baudrand, "Analysis of multilayer microstrip antennas by using iterative method," *Journal of Microwaves and Optoelectronics*, Vol. 3, No. 1, April 2003.
8. Zhang, R. and R. R. Mansour, "A novel lowpass microstrip filter using metal-loaded slots in the ground plane," *IEEE MTT-S. Microwave Symp. Dig.*, 1311–1314, June 2004.
9. Li, M., L. Haiwen, A. Boutejdar, W. Shuxin, and F. Tong, "Novel microstrip bandpass filter with slotted hexagonal resonators and capacitive loading," *Proc. 38th European Microwave Conference 2008 (EuMC)*, Amsterdam RAI, Amsterdam, The Netherlands, October 27–31, 2008.